Auditory Brainstem Responses in Two Closely Related *Peromyscus* Species (*Peromyscus leucopus* and *Peromyscus maniculatus*)

Luberson Joseph[1] (0009-0009-3805-2176), Emily Margaret New[1], Desi Marie Joseph[1](0009-0002-7612-9217), Tamara Chenell Woodley[1], Vanessa Yamileth Franco[1], Ben-Zheng Li[2] (0000-0002-8051-6212), Guinevere OU Wogan[1](0000-0003-1877-0591) and Elizabeth A. McCullagh[1*] (0000-0003-3779-0141)

[1]Oklahoma State University (OSU), Department of Integrative Biology, College of Arts and Sciences, Stillwater, Oklahoma 74078, USA
[2]University of Colorado Anschutz Medical Campus, Department of Physiology and Biophysics, Aurora, Colorado 80045, USA

*Corresponding author: elizabeth.mccullagh@okstate.edu
501 Life Sciences West, Stillwater, OK 74074 USA

ABSTRACT

The genus *Peromyscus* has been extensively used as a model for ecological, behavioral, and evolutionary studies. We used auditory brainstem responses (ABRs), craniofacial morphology, and pinna measurements to compare characteristics that could impact the threshold, amplitude, and latency of ABRs in two wild-caught species, *P. leucopus* and *P. maniculatus*. We observed significant differences in craniofacial and pinna attributes between species, with *P. leucopus* exhibiting larger features and bigger overall size compared to *P. maniculatus*. ABR recordings showed similar hearing thresholds with peak sensitivity between 8 to 46 kHz for both species. We found that amplitude of ABR wave I and IV increased significantly with increasing intensity, while no main effect of species was detected. Latency of wave I and IV significantly decreased with increasing intensity in both species. Finally, we observed longer latencies of the binaural interaction component (BIC) at longer interaural time differences (ITDs) in *P. leucopus*, while no differences were observed across relative BIC amplitude between species. These results

provide additional ABR related data that expands the use of both *Peromyscus* species as future models for auditory research.

Keywords: Binaural hearing, *Peromyscus*, Auditory brainstem recording, Pinna, Interaural timing difference (ITD)

INTRODUCTION

Auditory perception and sound localization are essential abilities for survival and fitness across diverse taxa. In small mammals, these abilities facilitate predator avoidance, capturing prey, finding mates, foraging, and conspecific communication (Colburn et al., 1987; Grothe et al., 2010; Kidd et al., 1995). To perceive sound source location, mammals rely on interaural time differences (ITDs) and interaural level differences (ILDs) between the two pinnae. ITD and ILD cues are influenced by the size of the head and the shape of the pinna (Blauert, 1997; Grothe et al., 2010). The auditory brainstem consists of specialized regions that integrate ITD and ILD information from the two ears. Despite decades of research on auditory perception and sound localization in rodent model species (Blauert, 1997; Grothe et al., 2010; Heffner, 2001), our understanding of species-specific biological variation in sound localization and hearing continues to need to be explored (Capshaw et al., 2023).

To understand the mechanisms of hearing, animal models, including laboratory and wild rodents, can serve as valuable tools. Most studies have used the laboratory house mouse (*Mus musculus*) as a model in hearing research due to its sensitive hearing, breeding success and maintanence in laboratory settings, and genetic manipulability (Capshaw et al., 2022; Ehret and

52 Dreyer, 1984). Yet, the limited genomic diversity in inbred laboratory rodents pose challenges to
53 fully recapitulating the broad spectrum of human disorder phenotypes (Voelkl et al., 2020). The
54 house mouse has faced criticism as a model for auditory research, owing to its poor sensitivity to
55 low frequency sounds, increased vulnerability to noise, short lifespan, and audiometric variation
56 within strains (Capshaw et al., 2022, Dammann, 2017). However, the auditory field has
57 leveraged many alternative species including the Mongolian gerbil (*Meriones unguiculatus*),
58 which is valued for its similarity of hearing range to humans (Heeringa et al., 2020; Jüchter et al.,
59 2022; Mills et al., 1990). Although these model taxa have shed insights in understanding the
60 fundamental mechanism of hearing, it is essential to continue to consider comparative
61 approaches that include a wider range of species, particularly those that reflect natural diversity
62 in their vocalizations, have long life spans, and vary in habitat use (Capshaw *et al* 2023).
63
64 The white-footed mouse (*Peromyscus leucopus*) and the North American deer mouse
65 (*Peromyscus maniculatus*) are two of the most abundant rodents in North America (Kirkland and
66 Layne, 1989). They both belong to the family Cricetidae and are more closely related to hamsters
67 and voles than to mice of the family Muridae. Both species have been extensively studied as
68 model systems in behavioral, biogeographical, developmental, ecological and evolutionary
69 investigations with regard to their physiological adaptation to varying habitat types (arboreal
70 habitats, grassland, woodlands, brushlands, swamps, and desert), their social system (mainly
71 promiscuous), and behaviors (maternal, winter nesting, climbing, and agonistic behaviors)
72 (Bedford and Hoekstra, 2015; Harney and Dueser, 1987; Lewarch and Hoekstra, 2018). Both
73 species are also of human health concern with regards to their carrying viruses and pathogens
74 including hantavirus, leptospirosis, and plague (Childs et al., 1994; Larson et al., 2018).

The two species differ in their body mass with *P. leucopus* displaying larger body mass and pinna (Light et al., 2021; Kamler et al., 1998). The average body mass of *P. leucopus* was reported to be 26.4 (± 3.9) and that of *P. maniculatus* was 14.5 (± 2.6) (Kamler et al., 1998). *Peromyscus* species hear best between 8 to 16 kHz, as demonstrated by low behavioral and ABR thresholds, with the ability to hear up to 65 kHz (Capshaw et al., 2022; Dice and Barto, 1952; Ralls, 1967). Differences in size may contribute to differences in hearing since pinna size impacts hearing by enhancing sound collection and amplification, improving frequency discrimination, and facilitating more accurate sound localization (Heffner et al., 2020; Heffner and Heffner, 1982).

Recently, members of the genus *Peromyscus* have emerged as valuable model systems in the field of neuroscience for studying age-related hearing loss due to their considerable lifespan compared to mammals of similar size (Capshaw et al 2022). *Peromyscus* species exhibit an average lifespan nearly double that of *M. musculus* when reared in laboratory settings, with the potential to live up to eight years (Burger and Gochfeld, 1992; Guo et al., 1993). In comparison to *M. musculus*, *Peromyscus* rodents display lower production of reactive oxygen species and enhanced resistance to oxidative stress, resulting in delayed accumulation of oxidative damage to deoxyribonucleic acid over the *Peromyscus* lifespan (Csiszar et al., 2007; Labinskyy et al., 2009; Shi et al., 2013), among other preventive effects which may slow cochlear aging (Ohlemiller and Frisina, 2008). Therefore, members of the genus *Peromyscus* show promise as models that can be used to complement auditory research across species and consequently can be reference taxa to explore small mammals' hearing across longer lifespans.

98 The purpose of this investigation is to compare hearing-related anatomy, hearing range,
99 monaural and binaural hearing of *P. leucopus* and *P. maniculatus* measured by craniofacial
100 features, pinna size, and auditory brainstem responses (ABRs). We expect that *P. maniculatus*
101 will have shorter binaural latency compared to *P. leucopus*, due to smaller overall body mass,
102 pinna, and craniofacial measurements. We also expect that there will be differences in other
103 measures of hearing including frequency thresholds and monaural ABRs (monaural amplitude
104 and monaural latency) due to differences in body mass, craniofacial features, and other
105 variability between these two closely related species.

106

107 **MATERIALS AND METHODS**

108 All procedures used for all experiments complied with the guidelines of the American
109 Society of Mammologists (Sikes and the Animal Care and Use Committee of the American
110 Society of Mammalogists, 2016), were approved by the Oklahoma State University Institutional
111 Animal Care and Use Committee (IACUC), and were conducted with permission from the
112 Oklahoma Department of Wildlife Conservation.

113

114 **Animals**

115 Experiments were conducted on 26 individuals, including 15 wild *P. leucopus* (9 males, 6
116 females) and 11 wild *P. maniculatus* (9 males, 2 females). Animals were live trapped using
117 aluminum Sherman (H.B Sherman Traps, Inc. Tallahassee, FL) non-folding traps (3” x 3” x 10”)
118 between June 2021 and July 2022 at three different locations across Oklahoma, USA
119 (Packsaddle Wildlife Management Area, James Collins Wildlife Management Area, and Payne
120 County) (Figure 1). The traps were baited with old fashioned oats and creamy peanut butter, left

overnight, and collected the next morning (~12 hours). Upon capture, animals were aged based on size, morphologically identified to species in the wild according to (Caire, 1989) and confirmed with Deoxyribonucleic acid (DNA) barcoding polymerase chain reaction (PCR) of collected tail snips. Age was estimated for each animal based on body mass and were divided into three age groups (juvenile, subadult, and adult) (see Table 1). Animals were then transported to the laboratory for ABRs.

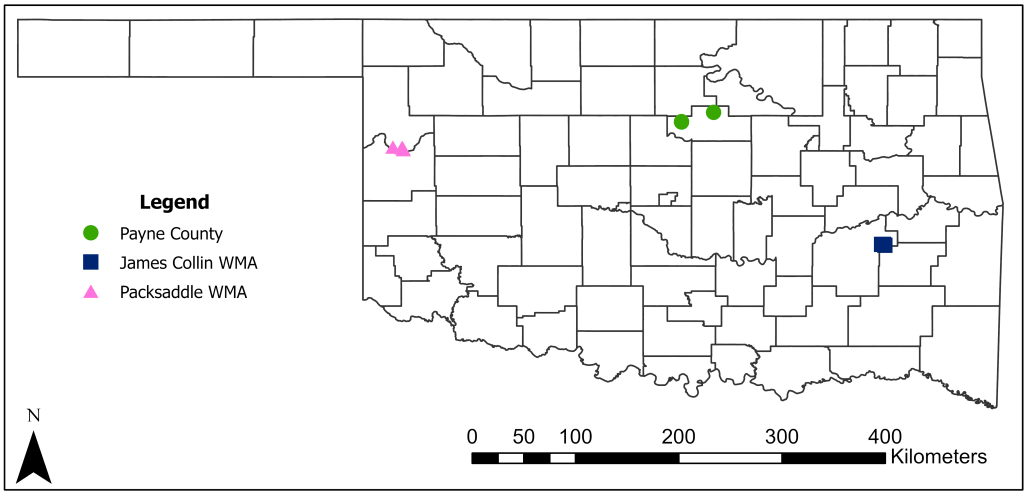

Figure 1: Map showing trapping site locations in Oklahoma. Packsaddle wildlife management area (WMA) sites are represented by pink triangles, James Collin wildlife management area (WMA) sites are represented by blue squares, and Payne County sites are represented by green circles.

DNA extraction, amplification, and sequencing

DNA was extracted from tail tissue samples by proteinase K digestion using a Qiagen DNeasy blood and tissue kit (Hilden, Germany) and the protocol outlined by (Nicolas et al., 2012). The DNA concentration and purity were first determined by using a Thermo Scientific Nano-Drop Lite-Spectrophotometer (Fisher Scientific, Spectrophotometer, Nanodrop Lite 6V

138 18W, Wilmington, DE). The Cytochrome c Oxidase Subunit I (COI) gene was amplified using
139 the primer sequences (CCTACTCRGCCATTTTACCTATG) and
140 (ACTTCTGGGTGCCAAAGAATCA) (Ducroz et al., 2001; Robins et al., 2007). DNA samples
141 were assayed in a 50 µl reaction with 25 µl Phusion Master mix, 2.5 µl forward primer, and 2.5
142 µl reverse primer and mQ water. The PCR comprised of 35 cycles: 95° C for 300 seconds; 30
143 seconds at 94° C, 40 seconds at 55° C, 90 seconds at 72° C, and a final 300 second extension at
144 72° C. The double-stranded PCR products were purified and sequenced at the Center for
145 Genomics and Proteomics of Oklahoma State University (Stillwater, Oklahoma, USA). All
146 sequences were compared with other COI sequences using the NCBI GenBank (Sayers et al.,
147 2022, 2021) databases to confirm species identification (supplemental Figure 1, supplemental
148 Table 1).
149
150 **Morphological measures**
151 Craniofacial morphology features including pinna size, tail length, body length, and body
152 mass were recorded for each animal using a six-Inch Stainless Steel Electronic Vernier Caliper
153 (DIGI-Science Accumatic digital Caliper Gyros Precision Tools Monsey, New York, USA) and
154 a digital stainless Steel Electronic scale (Weighmax W-2809 90 LB X 0.1 OZ Durable Stainless
155 Steel Digital Postal scale, Chino, California, USA). Measurements of animal head and pinna
156 including inter-pinna distance (mm) (measurement between the two ear canals), nose to pinna
157 distance (mm) (measurement from the tip of the nose to the middle of the pinna), pinna length
158 (mm) (basal notch to tip, excluding hairs), and pinna width (mm) were measured. Pinna
159 measurements (pinna width and pinna length) were used to calculate the effective pinna diameter
160 which is the square root of the pinna length multiplied by the pinna width (Anbuhl et al., 2017).

161 Tail length (sacrum to caudal tip, excluding hairs), body length (tip of nose to caudal tip), and
162 weight to the nearest gram were taken for each animal (Figure 2A). To assess dependence of
163 morphological traits on body size, log values of traits (pinna width, length etc.) were plotted
164 against the log body length (supplemental Figure 2).
165

166 **ABRs recordings**

167 We recorded ABRs from wild *P. leucopus* and *P. maniculatus* using similar procedures
168 as previous publications (Chawla and McCullagh, 2022; McCullagh et al., 2020; New et al.,
169 2024). Rodents were sedated with an intraperitoneal injection of 60 mg/kg ketamine and 10
170 mg/kg xylazine for initial anesthesia followed by maintenance dosage of 25 mg/kg ketamine and
171 12 mg/kg xylazine. After being fully sedated, as indicated by lack of toe pinch reflex, the
172 animals were transported to a small sound-attenuating chamber (Noise Barriers, Lake Forest, IL,
173 USA), and positioned on a water pump heating pad (set to 37° C). Subdermal needle electrodes
174 were inserted under the skin at midline between the ears over the brainstem (apex, active
175 electrode), directly behind the apex on the nape (reference), and in the back leg of the sedated
176 animals (ground electrode) for differential recordings. To obtain and amplify evoked potentials
177 from electrodes positioned below the skin of the animal, we used a Tucker-Davis Technologies
178 (TDT, Alachua, FL, USA) RA4LI head stage, a RA16PA preamplifier, and a Multi I/O processor
179 RZ5 attached to a PC with custom Python software to record the data. Data were processed using
180 a second order 50-3000 Hz filter and averaged across 10-12 ms of recording time over 500-1000
181 repetitions. Acoustic stimuli were delivered using TDT Electrostatic Speakers (TDT EC-1) for
182 frequencies between 32 and 64 kHz or a TDT Electrostatic Speaker-Coupler Model (TDT MF-1)
183 for clicks and frequencies ranging from 1 to 24 kHz. Speakers were coupled with custom ear

184 bars fitted with Etymotic ER-7C probe microphones (Etymotic Research Inc., Elk Grove Village,
185 IL) for in-ear calibration prior to recording for each animal. Tone stimuli were 4 ms in total
186 duration with a 1 ms on-ramp and 1 ms off-ramp (2 ms ± 1 ms on/off ramps). Click stimuli were
187 0.1 ms in duration with alternating polarity. Acoustic stimuli were presented to the animal with a
188 30 ms interstimulus interval with a standard deviation of 5 ms (Laumen et al., 2016a).
189 Randomizing interstimulus interval between each presentation has been shown to optimize the
190 ABR waveform (Wang et al., 2020). Stimuli were produced at a sampling rate of 97656.25 Hz
191 through a TDT RP2.1 real-time processor controlled by a custom Python program.
192
193 **ABR response threshold**
194 ABR response thresholds were determined by using the visual technique outlined by
195 (Brittan-Powell and Dooling, 2004). In short, threshold was defined to be between the intensity
196 at which the waveforms were no longer present and the previous intensity at which they were
197 visible in 5- and 10-dB increments specifically as absence of waveforms evoked by both left and
198 right monaural stimuli (i.e. complete absence of both waves, 5 dB increments were used when
199 near threshold). This method was used for analyzing the audiogram across frequencies presented
200 (1, 2, 4, 8, 16, 24, 32, 46, 64 kHz) and intensities (90 - 10 dB SPL) in addition to click threshold.
201
202 **Monaural ABR recordings**
203 Evoked potentials were recorded independently for each ear in response to single-ear
204 click stimulation and measured based on peak amplitude (voltage from peak to absolute trough)
205 and latency (time to peak amplitude) across the four peaks of the auditory brainstem recording
206 waveforms (Chawla and McCullagh 2022). To calculate the monaural latency and amplitude for

207 each species, we calculated the average of the monaural peak amplitude or latency of waves I
208 and IV from the ABRs data obtained for sound presentation in each ear across intensities (60-90
209 dB SPL) (New et al., 2024; Zhou et al., 2006).
210
211 **Binaural auditory brainstem response recordings**
212 To produce the binaural ABR response, we played broadband alternating polarity click
213 stimuli simultaneously or with an ITD at 90 dB SPL to both pinnae of the sedated animal. The
214 binaural interaction component (BIC) of the ABR was determined by subtracting the sum of the
215 two monaural auditory brainstem evoked responses from the binaural ABR recordings
216 (Benichoux et al., 2018; Laumen et al., 2016a). Custom Python software was used to measure the
217 BIC amplitude and latency, with amplitude calculated to the baseline of the recording (Chawla
218 and McCullagh, 2022). BIC was defined as the negative peak wave (DN1) at wave IV of the
219 ABR after subtraction of the summed monaural and binaural responses (See New *et al.* 2024 for
220 more details). To calculate how BIC varies with ITD, both species were presented with click
221 stimuli with shifting ITDs of -2.0 to 2.0 ms in 0.5 ms steps. We calculated the peak latency and
222 amplitude of DN1 at each ITD for each species. The ITD latency shift of the DN1 component of
223 the BIC was determined in relation to the latency of DN1 at 0 ITD. The DN1 amplitude is
224 highest at 0 ITD therefore amplitude for ITD shifts was transformed to relative amplitude with
225 respect to 0 ms ITD to normalize recorded data (Laumen et al., 2016a). The average latency shift
226 and relative DN1 amplitude values were used to make comparisons of binaural ABR as a
227 function of ITD between species.

228

229 **Statistical analyses**

230 All analyses and figures were created in R Studio version 4.0.3 (R Core Team 2020),
231 using ggplot2 (Wickham, 2016) and lme4 (Bates et al., 2014) packages. Two-way analysis of
232 variance (ANOVA) was used to statistically compare morphological characteristics between
233 species. Log-transformed morphological features (pinna width, length, etc.) were compared with
234 log body length and slope of the linear fit to describe potential allometry (slope > 1 indicating
235 positive allometry and < 1 indicating negative allometry). Data were analyzed using linear
236 mixed-effects models (LMMs) to account for repeat observation within one animal with species,
237 sex, frequency, peak, percentage relative DN1 amplitude, and shifts in DN1 latency of the BIC
238 as fixed effects and animal as random effect. If there were significant main effects of a variable
239 of interest, estimated marginal means were used for pairwise comparisons (Russell, 2018). To
240 control for multiple comparisons, emmeans implements a Tukey method for contrasts.

241

242 **RESULTS**

243 Based on the NCBI GenBank species identification systems for COI, of the tail samples
244 from the 26 animals collected, 15 individuals were identified as *P. leucopus*, and 11 as *P.*
245 *maniculatus* (supplemental table 1, Figure 1). *P. maniculatus* body length ranged from 55 to 78
246 millimeters (mm) with mean body mass of 12 grams (g), while *P. leucopus* body length ranged
247 from 65 to 93 mm with mean body mass of 21 g (Table 1).

248

Species	Age group	Body mass range (g)	Sample size (male, female)
P. maniculatus	Juvenile	< 14	8 (7, 1)
	Subadult	14 – 17	0
	Adult	> 17	3 (2, 1)

P. leucopus	Juvenile	< 13	1 (1,0)
	Subadult	13 – 18	4 (3, 1)
	Adult	> 18	10 (5, 5)

Table 1: Age was estimated based on body mass for each species based on published literature. Ages for *P. maniculatus* were described as follows: Juveniles < 14 g, subadults, between 14-17 g, and adults, > 17 g (Fairbairn, 1977). We inferred ages for *P. leucopus* as follow: Juveniles < 13 g, subadults, between 13 – 18 g, and adults > 18 g (Cummings and Vessey, 1994). We did not make comparisons by age due to limited sample sizes of each age group.

Morphological characteristics

Previous studies have shown that *P. leucopus* and *P. maniculatus* have significant differences in pinna sizes and craniofacial features (Choate, 1973; Light et al., 2021; Millien et al., 2017). We observed significant statistical differences for pinna attributes including pinna width (Df = 1, 24; F = 8.47; p = 0.0076) and pinna length (Df = 1, 24; F = 11.79; p = 0.0021) (Figure 2B and 2C respectively). In general, *P. leucopus* had longer and wider pinnae compared to *P. maniculatus*, with mean pinna length and width of 15.30 and 8.02 mm for *P. leucopus* and 13.15 and 6.42 mm for *P. maniculatus*. Similarly, effective pinna diameter (Df = 1, 24; F = 13.69; p = 0.0011) was significantly different between species, with *P. leucopus* having a wider effective pinna diameter compared to *P. maniculatus* (Table 2, Figure 2D). Craniofacial features including inter-pinna distance (Figure 2F; Df = 1, 24; F = 9.08; p = 0.0060) and distance from the nose to the pinna (Figure 2E; Df = 1, 24; F = 5.82; p = 0.0239) were significantly different between species with *P. leucopus* exhibiting a wider distance between pinnae and a longer distance from the nose to the pinna. Like pinnae morphology and craniofacial features, there were significant differences in body mass (Df = 1, 24; F = 24.2; p = 0.00005 , Figure 2I), tail length (Df = 1, 24; F = 25.76, p = 0.0245, Figure 2H), and body length (Df = 1, 24; F = 18.32; p = 0.0002, Figure 2G) between both species, with *P. leucopus* weighing significantly more including longer tails and longer body length than *P. maniculatus* (Table 2). We tested if there

were sex differences in craniofacial and pinna sizes in *P. leucopus*. There were no significant differences in craniofacial and pinna sizes between male and female *P. leucopus* (all p-value > 0.05). Sex differences were not explored for *P. maniculatus* due to limited number of female subjects of this species (9 males, 2 females). When anatomical data were compared for potential effects of body size (allometry), log features (pinna width, etc.) compared to log body length did not show positive allometry except for tail length, which indicated positive allometry (slope of 1.437 (*maniculatus*) and 1.218 (*leucopus*), supplemental Figure 2).

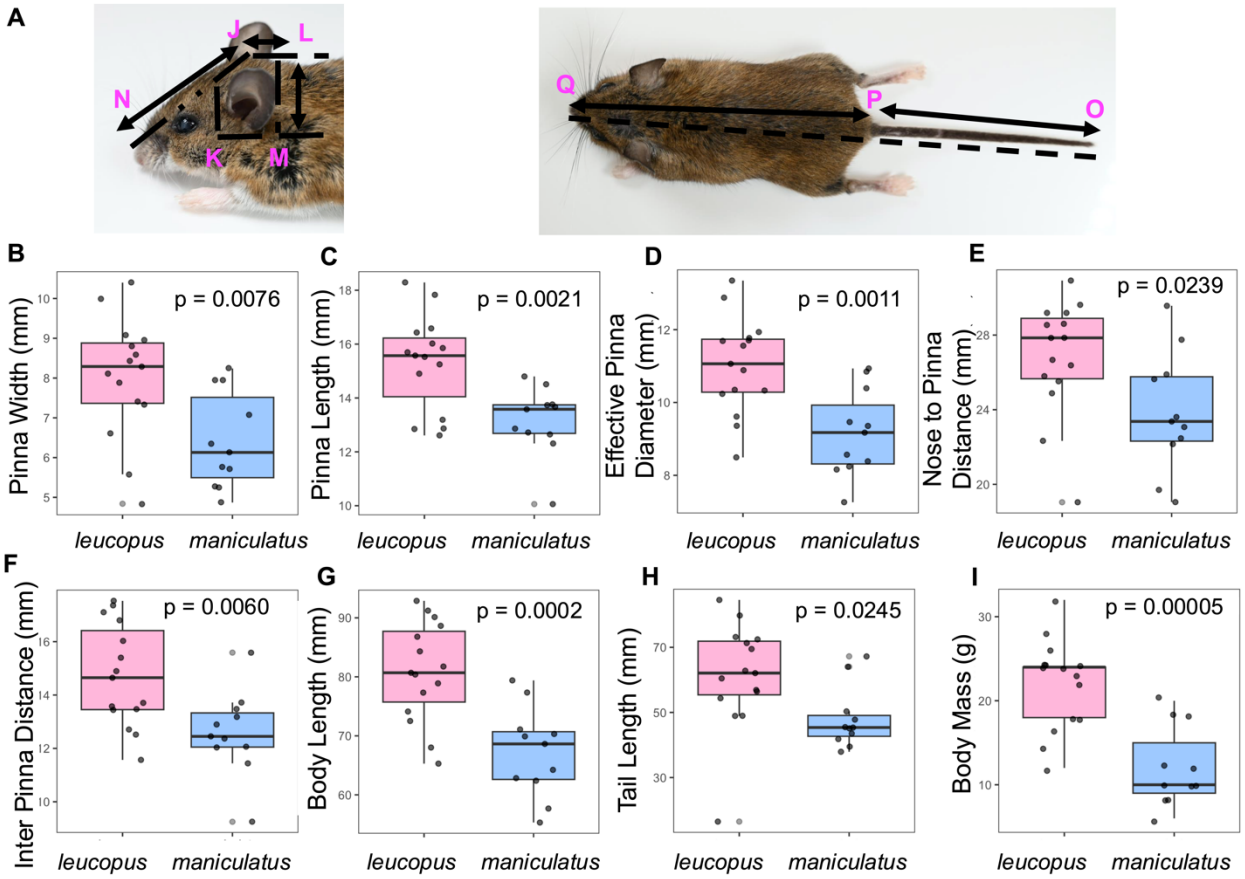

Figure 2: Morphological differences between *P. leucopus* and *P. maniculatus*. Pinnae, head, and body features (**A**) were evaluated between species (pink boxplot = *leucopus*, blue boxplot = *maniculatus*). Measurements JK show the inter pinnae distance, JN the nose to pinna distance, MK the pinna width, LM the pinna height, OP the tail length, and PQ the body length. Effective pinna diameter was calculated by taking the square root of pinna height multiplied by pinna width (MK/LM). Significant differences were observed for all features including Pinna width (**B**), Pinna length (**C**), Effective diameter (**D**), Nose to

289 pinna distance (**E**), Inter pinna distance (**F**), Body length (**G**), Tail length (**H**), and Body mass (**I**).
290 Peromyscus pictured is a wild caught *P. leucopus* captured in Payne County, Stillwater, Oklahoma. Image
291 is presented only for demonstration of measurements.
292
293

Morphological characteristics	*Maniculatus* mean ± S. E	*Leucopus* mean ± S. E	degrees of freedom	F-statistic	p-value
Effective pinna diameter	9.16 ± 0.36	11.01 ± 0.34	1, 24	13.69	0.0011
Pinna length	13.15 ± 0.39	15.30 ± 0.45	1, 24	11.79	0.0021
Pinna width	6.42 ± 0.36	8.02 ± 0.39	1, 24	8.47	0.0076
Inter pinna distance	12.59 ± 0.47	14.72 ± 0.49	1, 24	9.08	0.0060
Nose to pinna distance	23.84 ± 0.96	26.82 ± 0.79	1, 24	5.82	0.0239
Body length	67.19 ± 2.28	80.87 ± 2.17	1, 24	18.32	0.0002
Tail length	48.01 ± 2.84	61.21 ± 4.21	1, 24	25.76	0.0245
Body mass	12.0 ± 1.0	22.0 ± 1.0	1, 24	24.2	0.00005

294
295 **Table 2:** Morphological characteristics features of *P. maniculatus* and *P. leucopus* of the Packsaddle
296 wildlife management area (WMA), James Collin wildlife management area (WMA) and Payne County.
297 Values presented represent the mean of different morphological features recorded ± standard error, the
298 degrees of freedom, F-statistic, and p-value of morphological differences between species.
299

300 **ABR thresholds between species**

301 Both *P. maniculatus* and *P. leucopus* displayed the best sensitivity to tones between 8 to
302 46 kHz, as indicated by lower ABR thresholds (below 55 dB SPL, Figure 3C). We detected no
303 significant statistical difference in ABR frequency threshold between species across the
304 frequencies tested (LMM, p = 0.543). Similarly, no significant difference in ABR frequency
305 hearing threshold was observed between male and female *P. leucopus* (LMM, p = 0.523). We
306 next investigated whether craniofacial or pinna measurements features are correlated with or
307 influence ABR frequency thresholds in both species. We found that none of the morphological

measurements had a significant effect on ABR frequency hearing thresholds between species (all $p > 0.05$) (supplemental materials, Figure 3,4,5).

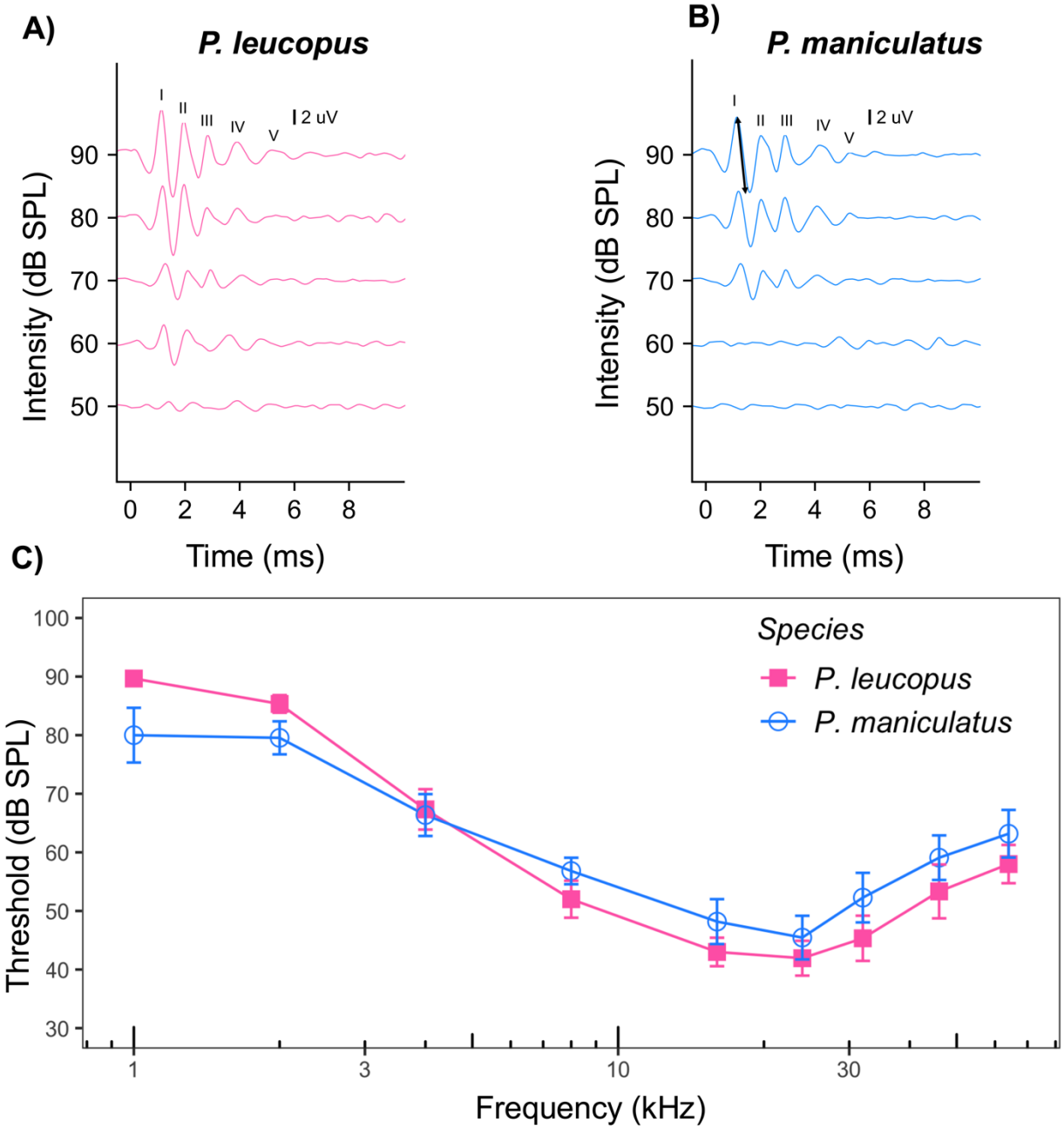

Figure 3: Figure 3A and 3B show auditory brainstem response patterns of a female *P. leucopus* (left) and a female *P. maniculatus* (right) determined with clicks of different intensities. Main waves I-V are identified in the 90 dB SPL example. Hearing range was measured across frequency (1-64 kHz) for both *P. leucopus* and *P. maniculatus* (Figure 3C). The vertical bars represent the standard error at each frequency. (Figure 3C). No significant main effects of frequency between species were found. Unfilled blue circles represent *P. maniculatus* while filled pink squares represent *P. leucopus*. Arrow in figure 3B shown how ampliture were calculated.

318

319 **ABR waveform amplitudes**

320 The amplitude of individual ABR waves was measured as the difference between the
321 positive peak and the following negative trough (as shown by the arrow in Figure 3B). At 90 dB
322 SPL, the average amplitudes of wave I and wave IV were 4.75 and 2.25 μV for *P. leucopus*. For
323 *P. maniculatus*, the average amplitudes of wave I and wave IV were 5.87 and 2.13 μV at 90 dB
324 SPL. We observed that the amplitude of waves I and IV (*P. maniculatus*: Figure 4A and 4C,
325 wave I and IV unfilled circles; *P. leucopus*: Figure 4B and 4D, wave I and IV filled squares),
326 increased monotonically with increasing intensity (60 to 90 dB SPL). Linear mixed-effect
327 models revealed a significant main effect of intensity on the amplitude for both waves (LMM: p
328 < 0.0001). However, no significant main effect of species was detected on the amplitude for both
329 waves (LMM: wave I $p = 0.289$, wave IV $p = 0.674$). Similarly, a significant main effect of
330 increasing intensity on peak amplitude for wave I and wave IV between male and female *P.*
331 *leucopus* (LMM: $p < 0.0001$). However, there was no significant main effect of sex on monaural
332 wave I and IV amplitude with increasing intensity for *P. leucopus* (LMM: $p = 0.851$).

333

334 **Monaural Amplitude Ratio**

335 Monaural amplitude ratio was calculated by dividing the amplitude value of wave IV by
336 the amplitude value of wave I for left and right pinnae at each intensity. For both species, wave
337 IV (4C and 4D) overall had smaller amplitude than wave I (Figure 4A and 4B) and as a result,
338 the wave IV/I amplitude ratio was generally lower than 1.0 at most intensities tested in both
339 species (Figure 4E, *P. leucopus*: filled squares and *P. maniculatus*: unfilled circles). The results
340 of the linear mix-effect model revealed no significant main effects of either intensity (LMM: p =

341 0.158) or species (LMM: p = 0.567) on the amplitude ratio of wave I and IV. Similarly there was

342 no main effect of either intensity (LMM: p = 0.465) or sex (LMM: p = 0.705) for *P. leucopus* on

343 the amplitude ratio of wave I and IV.

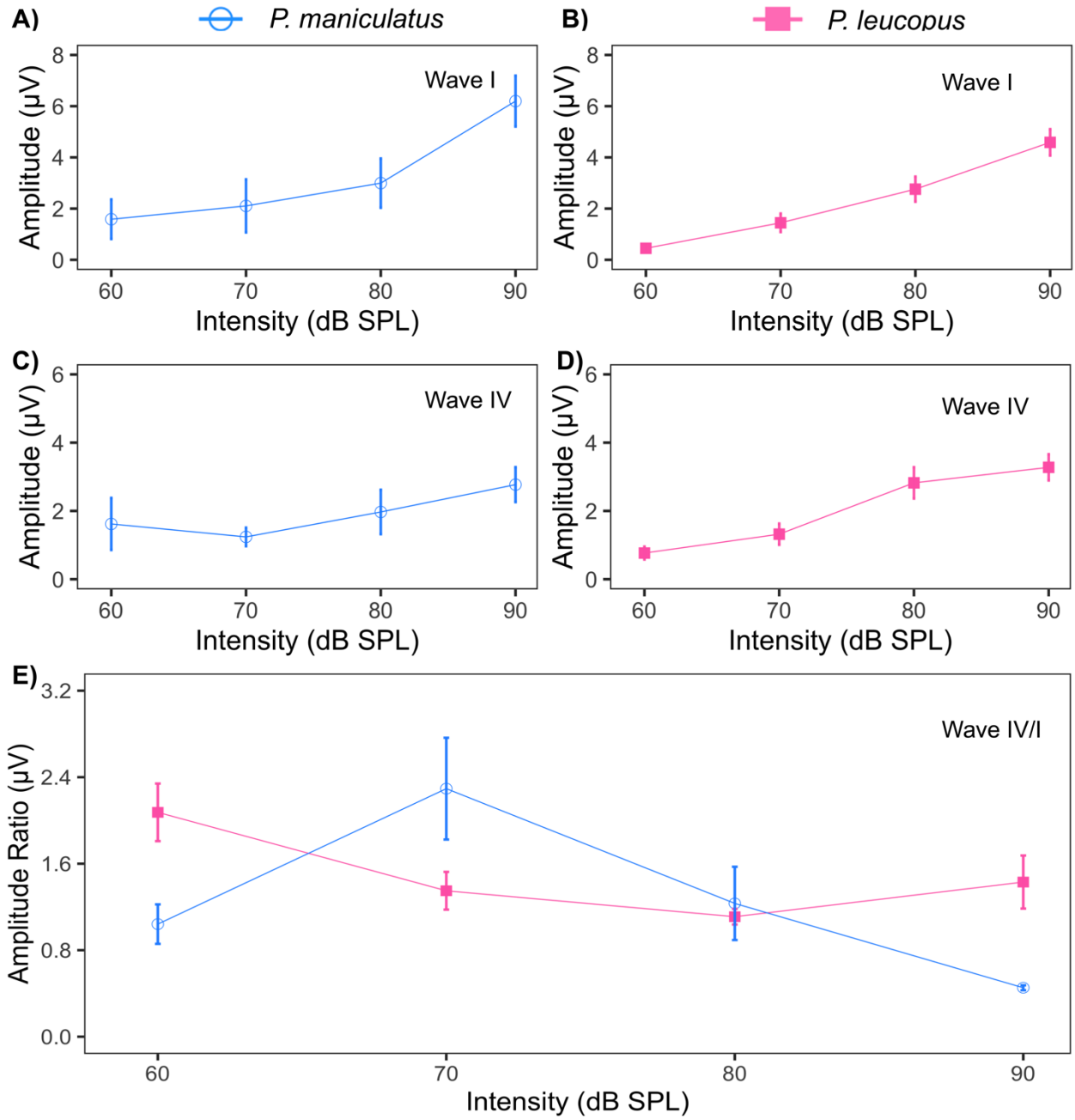

344

345 **Figure 4:** Average amplitude of wave I and wave IV of auditory brainstem responses determined with
346 clicks of different intensities (pink filled square = *P. leucopus* (n = 15), blue unfilled circle = *P. maniculatus*
347 (n = 11)). The average wave IV/I amplitude ratio at each intensity is shown in figure 4E. The vertical bars

348 represent the standard error at each point. Significant main effects of intensity on wave I and IV amplitude
349 were detected for both species.
350
351 **Absolute Latency**

352 Peak latency is the time interval between the presentation of a sound stimulus and the
353 peak at maximum amplitude of the designated wave. We calculated the average peak latency of
354 waves I and IV of both studied species across click intensities (60 to 90 dB SPL). Linear mixed-
355 effect models revealed a significant decrease in peak latency for both waves with increasing
356 intensity between species (Figures 5A, 5B, 5C and 5D, LMM: all $p < 0.0001$). There was a
357 significant main effect detected for species in peak latency for wave I (LMM: $p = 0.00276$), but
358 not wave IV (LMM: $p = 0.0797$) with increasing intensity. However, pairwise comparisons did
359 not show significance at a particular intensity suggesting that overall *P. maniculatus* had shorter
360 latencies, when considering all intensities, than *P.* leucopus for wave I only when using non-
361 relative measures (Figure 5A, 5B). Similarly, significant decreases in peak latency with
362 increasing intensity were observed for wave I and wave IV between male and female *P. leucopus*
363 (LMM: all $p < 0.0001$). There was a significant main effect of sex detected for wave I in *P.*
364 *leucopus* (LMM: $p = 0.0106$), driven by sex differences at 90 dB (LMM: $p = 0.0027$), with no
365 main effect of sex on wave IV (LMM: $p = 0.293$). We next determined the slope latency of ABR
366 waves between species by plotting the latency data of wave I and IV against different click
367 intensities of each species (Supplemental, Figure 6). The slope of wave I latency was - 0.02 for
368 *P. leucopus* and – 0.01 for *P. maniculatus*, while the slope of wave IV was – 0.03 for *P. leucopus*
369 and – 0.04 for *P. maniculatus*.
370
371 **Inter-peak latency**

Inter-peak latency was calculated as the difference in latency from the wave I peak to wave IV peak for left and right pinnae at each intensity, which provides a more relative measure for comparing between species. Because the decrease in peak latency with increasing intensity was more pronounced for wave IV than for wave I, the inter-peak latency between wave I and wave IV also showed a significant decrease as intensity increased, as illustrated in Figure 5E (LMM: $p = 0.00155$, pink filled squares = *P. leucopus*, blue unfilled circles = *P. maniculatus*). However, no main effect of species was detected on the inter-peak latency of waves I and IV between both species (LMM: $p = 0.281$). There was a significant decrease in wave I-IV inter peak latency with increasing intensity for male and female *P. leucopus* (LMM: $p = 0.0151$) however there was no main effect of sex (LMM: $p = 0.252$).

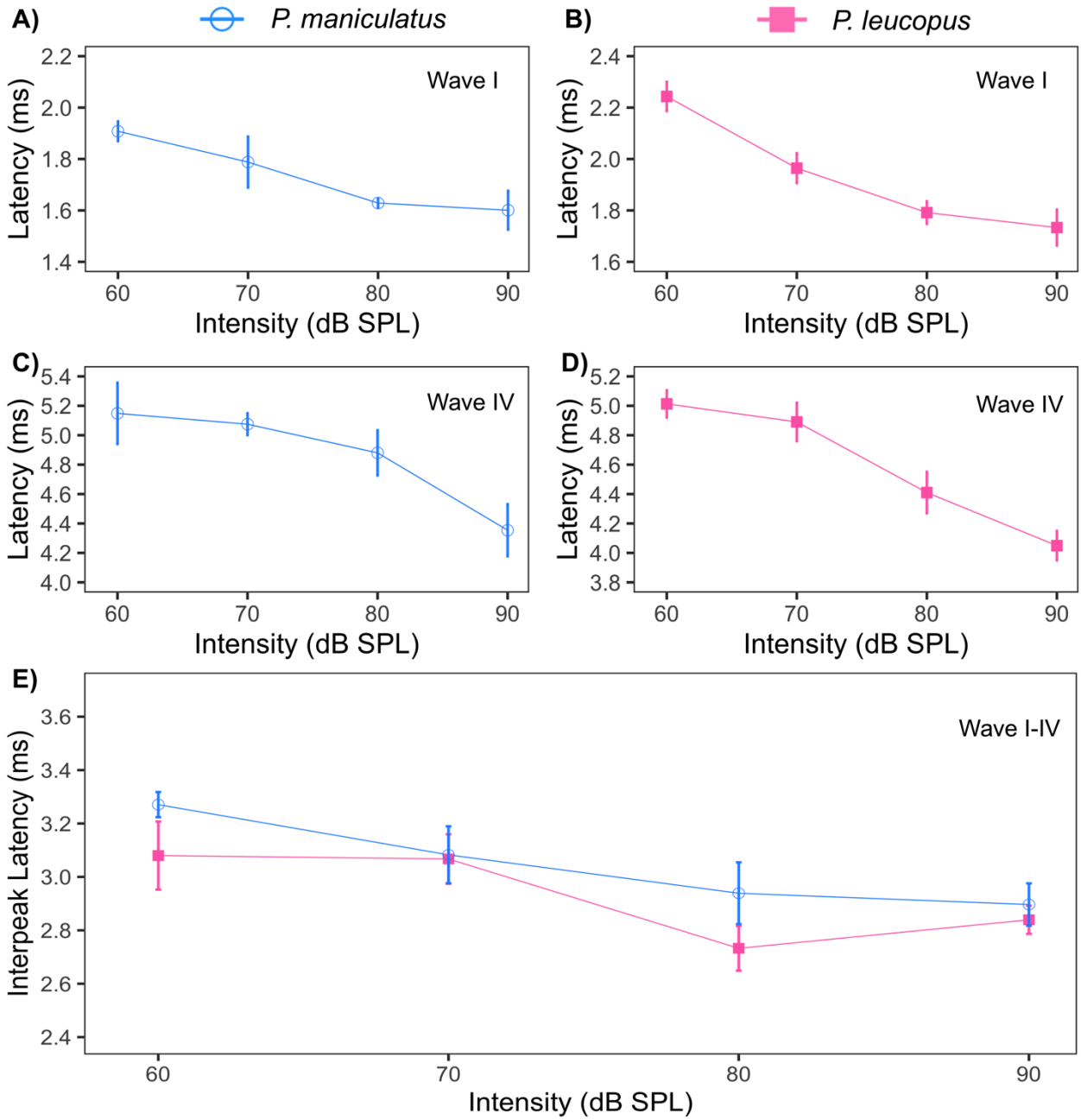

Figure 5: Average peak latency of wave I and wave IV of auditory brainstem responses determined with clicks of different intensities (Pink filled squares = *P. leucopus* (n = 15), Blue unfilled circles = *P. maniculatus* (n = 11)). The average wave I-IV inter-peak latency at each intensity is shown in 5E. The vertical bars represent the standard error at each point.

Binaural ABR measures

We used the latency shift of the DN1 component of the BIC and relative DN1 amplitude to show the relationship of ITD on latency and relative amplitude of the BIC across species. For both species, DN1 latency increased with longer ITDs and DN1 relative amplitude decreased with longer ITDs. The average DN1 amplitudes at 0 ITD were 2.72 μV and 1.74 μV for *P. maniculatus* and *P. leucopus*, respectively. The average latency for the DN1 component at 0 ITD was 5.0 ms for *P. maniculatus*, compared with 5.6 ms for *P. leucopus*. Linear mixed-effects models indicated significant main effects of ITD across relative DN1 amplitude (LMM: $p < 0.0001$), indicating that as ITD increased, relative DN1 amplitude decreased. No main effect of species was observed across relative DN1 amplitude (Figure 6B, LMM: $p = 0.818$). Similarly, there were significant main effects of ITD across relative DN1 amplitude between male and female *P. leucopus* (LMM: $p < 0.0001$), while no significant main effect of sex was detected (LMM: $p = 0.0929$). There were statistically significant main effects of both ITD (LMM: $p < 0.0001$) and species (LMM: $p < 0.0162$) in latency shift of the DN1 component of the BIC in relation to ITD normalized for 0 ITD between *P. maniculatus* and *P. leucopus* (Figure 6A). Shift in DN1 latency of the BIC was significantly faster in *P. maniculatus* compared to *P. leucopus* at 1.0 ms ($p = 0.0377$) and 2.0 ms ($p = 0.0222$) ITD (Figure 6A). There were significant differences in in latency shift of the DN1 component of the BIC in relation to ITD normalized for 0 ITD for male and female *P. leucopus* (LMM: $p < 0.0001$) but no main effect of sex (LMM: $p = 0.843$).

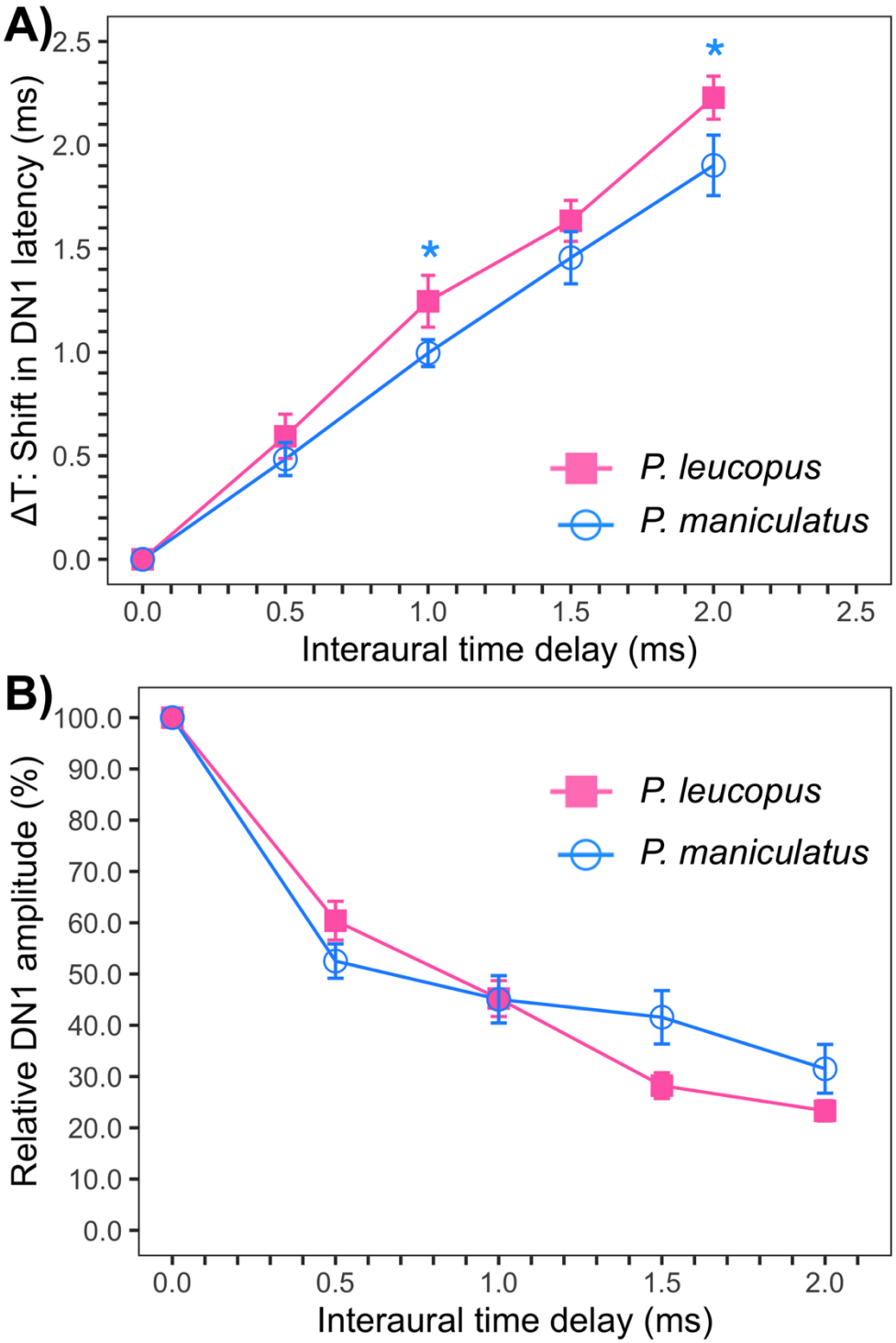

Figure 6: Binaural ABRs in wild *P. leucopus* (pink filled square) and *P. maniculatus* (blue unfilled circle). 6A, Shift in DN1 latency (ms) relative to ITD; reference latency at ITD = 0 is set to 0 ms. 6B, percentage relative DN1 amplitude relative to ITD normalized to the DN1 amplitude for ITD = 0 ms. Relative amplitude and latency of the DN1 BIC with varying ITD between - 2 to + 2 ms in 0.5 ms steps were measured. Significant main effects of ITD and species were detected in BIC shift in DN1 latencies between

both species. No significant main effect of species was observed for relative amplitude of the BIC across ITDs. The vertical bars represent the standard error at each ITD.

DISCUSSION

In this study, we used craniofacial morphology, pinna features, and ABRs to compare morphological features important for hearing with physiological measures of ABR amplitude and latency of two species of the genus *Peromyscus*. Like previous findings (Choate, 1973; Light et al., 2021; Millien et al., 2017), we detected significant morphological differences between species for all measurements (including pinna length, pinna width, etc.) with *P. leucopus* displaying larger features. ABR-derived detection thresholds revealed that both species share similar ABR response thresholds across frequencies with the lowest ABR frequency thresholds between 8-46 kHz, which is in agreement with previous findings that showed *Peromyscus* species have best hearing sensitivity between 8-16 kHz (Capshaw et al., 2022; Dice and Barto, 1952; Ralls, 1967). Significant main effects of intensity were detected in monaural amplitude of ABR wave I and IV between both studied species, which is similar to Zhou and colleague's findings using laboratory mouse strains (Zhou et al., 2006). Measurements of the BIC indicated significant main effect of ITDs on DN1 amplitude and latency between the two species. Significant main effect of species was detected for DN1 latency, but not for DN1 amplitude. Overall, our results revealed that both species have similar ABR hearing thresholds with *P. maniculatus* having shorter latency BIC and smaller anatomical features compared to *P. leucopus*.

Morphological features including cranial size and shape, size of the pinnae, body and tail length differ widely within species of the genus *Peromyscus* (Light et al., 2021; Ordóñez-Garza et al., 2010). Our data showed differences in all measured anatomical traits between species

consistent with previous studies (Choate, 1973; Light et al., 2021; Millien et al., 2017). Previous studies used two-dimensional (2D) geometric morphometrics (Light et al., 2021), and micro-CT (Riede et al., 2022) as tools to morphologically differentiate rodents of the genus *Peromyscus*. Light *et al* (2021) showed differences between *P. leucopus* and *P. maniculatus* based on head size, pinnae features, hindfoot length, and other morphological features similar to our study. Consistency in morphological features (pinna length, pinna width, and body weight) documented in this study provide additional evidence supporting the use of these morphology traits as reliable indicators for distinguishing species within the genus *Peromyscus*.

Using ABRs, Capshaw *et al.* (2022) observed low hearing sensitivity to frequencies below 2 kHz in two laboratory *Peromyscus* species (*P. leucopus* and *P. californicus*). Our findings are consistent with Capshaw *et al.* (2022), with hearing thresholds around 85 dB SPL at frequencies below 2 kHz in both studied species, suggesting relatively poor hearing sensitivity of both studied species to low frequencies. Small-headed mammals generally are not as sensitive to low frequencies and do not generate significant directional information with them due to minimal differences in timing and intensity between pinnae (Lauer et al., 2018). Therefore, it is thought that small mammals rely on high frequencies for directional hearing with exception of some subterranean mammals including the naked mole-rat (*Heterocephalus glaber*), the plain pocket gopher (*Geomys bursarius*), and the blind mole rat (*Spalax ehrenbergi*) that have poor sound localization and lack high frequency hearing (Heffner and Heffner, 1993, 1992, 1990), though see (Barker et al., 2021; Gessele et al., 2016; McCullagh et al., 2022). The limited ability of small mammals (with exception of Mongolian gerbils, chipmunks, groundhogs, hamsters, and others), like members of the genus *Peromyscus*, to detect low frequency sounds has been

465 attributed to selective pressure linked with the absence of cues for localizing sounds in the
466 horizontal plane for these small-headed animals (Heffner et al., 2001). Therefore, it is not
467 surprising that we did not observe low frequency sensitivity for the two studied species in the
468 current investigation.

469 *P. leucopus* and *P. maniculatus* are both highly territorial and produce both sonic and
470 ultrasonic vocalizations between 0.8 to 28 kHz (sustained vocalizations: frequency ranges
471 between 10-25 kHz, sweep vocalization: frequencies above 25 kHz, and barks: frequency ranges
472 between 0.8 and 6 kHz) (Miller and Engstrom, 2012; Pomerantz and Clemens, 1981; Riede et al.,
473 2022). The frequency ranges of ultrasonic vocalizations of both studied species correlate with
474 their frequency thresholds (Figure 3C, best frequency threshold ranging from 8 - 46 kHz).
475 Related species' (California mouse, *P. californicus*) defensive and distress vocalizations are
476 known to be associated with sounds ranging from 2 -30 kHz (Rieger and Marler, 2018). While
477 limited studies have described distress and defensive vocalizations across the genus *Peromyscus*,
478 previous investigations have reported that members of this genus produce agonistic calls such as
479 chits and barks at frequencies between 6 to 15 kHz (Houseknecht, 1968; Pasch et al., 2017).
480 These findings suggest a good match of *Peromyscus's* vocalization with their ABR threshold
481 sensitivity (8 – 46 kHz) likely contributing to vocal air-borne communication in the wild.

482 The white-footed mice (*P. leucopus*) and deer mice (*P. maniculatus*) occur throughout
483 Oklahoma but generally occupy different habitats, with *P. maniculatus* being more common in
484 grasslands and *P. leucopus* primarily inhabiting shaded forests (Hackney and Stancampiano,
485 2015; Stancampiano and Schnell, 2004). In our study, *P. leucopus* subjects were mainly captured
486 in shrubland and forested habitats, while *P. maniculatus* subjects were found in open grassland
487 habitats. Our findings revealed that *P. leucopus* has similar sensitivity to frequencies as *P.*

488 *maniculatus* across all frequencies tested. We may be missing potential species level difference
489 however due to suspected differences in age between the species. Weight distribution suggests
490 that eight of the 11 *P. maniculatus* subjects in the current study were juveniles, while 10 of the
491 15 *P. leucopus* were adults. Age differences may mask any potential species level differences, as
492 small shifts in audiogram thresholds have been observed in *P. leucopus* with aging (Capshaw et
493 al., 2022). A comparative study evaluating the vocalization content and sound propogation of
494 vocalizations of both species in their respective habitats, across different age groups, would shed
495 novel insights into how habitat-related factors and age might influence sound reception and
496 communication strategies both within and among closely related *Peromyscus* species.

497 Amplitude of wave I and IV tend to increase monotonically in most small mammals with
498 increasing intensity when measured by click stimuli (Zhou et al., 2006). Similar patterns have
499 been reported in other taxa commonly used in evoked potential studies (Backoff and Caspary,
500 1994; Neil J. Ingham, 1998). Though we didn't see any difference between the species for
501 relative wave amplitude, we did observe differences in craniofacial size and mass, however they
502 were proportional (larger animals had more mass and bigger pinna). Previous studies indicate
503 that smaller craniofacial size with small body mass may bring the recording electrodes into
504 closer proximity to the generators, resulting in larger amplitudes compared to those with large
505 body mass (Merzenich et al. 1983) though in our studies the disparities in size may not have been
506 large enough for this effect to be seen.

507 ABR wave amplitude can be affected by several factors including electrode position,
508 animal body temperature, external noise, recording protocol, and equipment characteristics,
509 therefore normalization between waves can help control for this variability. In humans, it has
510 been shown that auditory deficits related to retrocochlear pathology may lead to a decrease in

511 wave IV amplitude, and ultimately cause a decrease in the wave IV/I amplitude ratio (Arnold
512 2000). Our data revealed that the wave IV has a smaller amplitude than wave I in both species at
513 most intensities tested, resulting in a wave IV/I ratio less than 1.0 (Figure 4E). Previous work
514 measuring ABR in inbred mouse strains, rats, gerbils, cats, guinea pigs, and humans indicated
515 that the ABR waves I and II are generally larger amplitude than ABR waves III and IV, which is
516 in agreement to the current study (Moore, 1983). However, wave II and III are relatively larger
517 in rats and guinea pigs, while shifted to wave IV in cats and wave IV-V complex in humans
518 (Merzenich et al., 1983). Accordingly, the species-specific differences in individual ABR wave
519 amplitude may result from complex factors including the evolution of the central nervous
520 system, neuronal response characteristics within the brainstem, and neural conduction velocity.
521 ITD and ILD are two cues that animals with external pinnae use for sound localization.
522 ITDs are generally processed by neurons in the medial superior olive (MSO <2kHz) while ILDs
523 are mainly processed by neurons in the lateral superior olive (LSO >2 kHz) (Grothe et al., 2010;
524 Suzuki and Horiuchi, 1981). Previous studies reported that the mean DN1 amplitude at 0 ITD
525 was 0.2 μV in humans, about 5 μV in guinea pig, 1.8 μV in gerbil, and 2.3 μV in cats (Goksoy et
526 al., 2005; Jones and Van der Poel, 1990; Laumen et al., 2016a; Riedel and Kollmeier, 2006;
527 Ungan et al., 1997). Comparatively, the DN1 amplitude at 0 ITD of wild *Peromyscus* species is
528 similar to that of gerbils and cats, higher than that of humans and significantly lower than that of
529 guinea pig. Differences in DN1 amplitude at 0 ITD observed could be a result of smaller distance
530 of the recorded electrodes to the brainstem in small animals, as well as electrode configuration,
531 or other procedural differences.
532 Numerous publications have reported that latency of the DN1 component in humans
533 ranges from 5.6 to 6.8 ms, while those of other animal models (gerbil, cats, guinea pig) range

534 from 3.7 to 4.8 ms (Goksoy et al., 2005; Jones and Van der Poel, 1990; Riedel and Kollmeier,
535 2006; Ungan et al., 1997). Our data on the latency DN1 component is consistent with latencies
536 observed in humans and is somewhat slower than what is seen in other animal models. Our
537 results are similar with others that show the latency of the DN1 component increases with longer
538 ITDs in cats, gerbil, guinea pig, and humans (Goksoy et al., 2005; Laumen et al., 2016b; Riedel
539 and Kollmeier, 2006; Ungan et al., 1997). Indeed, it has been suggested that the increase in DN1
540 latency with increasing ITD reflects the anatomy and interaction between excitatory and
541 inhibitory neurons in the superior olivary complex (Karino et al., 2011).

542 We observed faster latencies of DN1 and wave I in *P. maniculatus* compared to *P.*
543 *leucopus*, (when not considering the relative interpeak latency for wave I). It is hard to speculate
544 whether the difference in DN1 latency observed between both species is associated with head
545 size or the number of cells in the superior olivary complex (SOC) nuclei. Studies characterizing
546 the number of excitatory and inhibitory cells in the SOC of both species would be beneficial to
547 allow for evaluation of the effects of head size or medial superior olive (MSO) and lateral
548 superior olive (LSO) size in shifts of the DN1 latency among *Peromyscus* species. Further
549 studies involving more *Peromyscus* species and other techniques, such as head-related transfer
550 functions, are needed to assess if larger external pinna sizes contribute to additional features of
551 *Peromyscus* hearing such as the use of spectral notches and the contribution of the pinna to
552 horizontal cues like ITD and ILD, particularly since our in-ear presentation of ITD stimuli
553 bypass the pinna. We calculated the functional interaural distance for each species by summing
554 the mean inter-pinna distance and pinna width divided by the speed of sound in air to evaluate
555 the availability of ITD cues for each species. While this technique is limited due to our use of
556 calipers and is not exactly the same as the time delay caused by sound traveling around the head,

557 we nonetheless used this to roughly estimate the functional interaural distance for each species.
558 We found that *P. maniculatus* have a shorter functional interaural distance (± 55 μs) compared to
559 *P. leucopus* (± 67 μs) which is consistent with smaller heads in *P. maniculatus*.
560 There are some limitations to the techniques employed in this study. Calipers are less
561 accurate as features get smaller due to their measurement sensitivity, therefore measures of pinna
562 and head morphology are likely to be less accurate than larger measurements such as body length
563 and tail length. We conducted analyses correcting for overall body length; however, they did not
564 show significant positive allometry (slope > 1) indicating that either these features were not
565 allometric or the loss of accuracy of measurements at smaller distances contributed significantly
566 to error. However, the one measurement that showed positive allometry was tail length, which is
567 one of the longer, or perhaps more accurate, measures suggesting that finer measurement tools
568 might be needed to make further arguments about effects of overall body size and morphological
569 features on hearing in these species. There are also limitations to using ABRs as measures of
570 hearing, including that interpretation of thresholds using visual observation, as performed in our
571 study, can be subjective (Suthakar and Liberman, 2019). However, others have shown minimal
572 differences between algorithms and observers to auditory threshold measurements (Capshaw et
573 al., 2022). Further validation of our observer method with more quantitative algorithms would be
574 useful to confirm threshold values reported here, though our thresholds coincide well with the
575 published literature in one of these species (Capshaw et al., 2022). Lastly, behavioral measures
576 of hearing can show differences compared to ABRs, and indeed anesthetics used, montage of
577 electrodes, calibration of sounds (in ear or other methods), sound presentation, and other factors
578 all may influence ABR results making cross-species and cross-publication results difficult to
579 interpret (Ramsier and Dominy, 2010; Wolski et al., 2003). However, the current study used the

same parameters across both species and showed results consistent with the literature and what might be expected for species that are closely related but differ primarily in size giving us confidence in the results presented here.

CONCLUSIONS

Our findings provide a deeper understanding of auditory similarities and differences between two species of *Peromyscus* and validate that the highly abundant *Peromyscus* may serve as a future model for auditory studies. Both species show differences in craniofacial and pinna features and exhibit best ABR thresholds at frequencies ranging from 8 to 46 kHz. *P. maniculatus* showed shorter relative latencies of the DN1 component of the BIC, while relative DN1 amplitude was not different between the species. Further physiological assessment exploring hearing between the sexes at different ages and across the lifespan are needed to further show whether there are differences in hearing under these conditions. In addition, clarifying the role of the BIC between sexes across species of the genus *Peromyscus* is important to understand its relevance for potential sex differences.

ACKNOWLEDGMENTS

We would like to thank Game wardens, Benny Farrar and Marcus Thibodeau for housing and giving us opportunities to sample at James Collin and Packsaddle Wildlife Management Areas. Also, we would like to thank members of team wild rodent of the McCullagh lab which helped in trapping and performed ABRs. We would also like to thank Dr. Tim Lei and Benzheng Li for their creation of the ABR acquisition and analysis custom python software. Dr. Fabio Machado helped with interpreting analyses of allometry and body size measurements. NSF

RaMP DEB 2216648, and Oklahoma State University College of Arts & Sciences (CAS) Research Program to EAM helped fund summer support, RA support for LJ and undergraduates involved in the project, and some materials (CAS research award). Support for VYF was provided by a Wentz and CAS AURCA program support, and EMN with Wentz fellowship support as well as additional support for LJ from the Payne County Audubon Society.

DATA AVAILABILITY

The data of the study will be made available upon request.

AUTHOR CONTRIBUTIONS

LJ, EMN, TCW, VYF, And DMJ captured the animals and LJ and EMN collected the ABR data for the manuscript. LJ, DMJ, and GOUW performed DNA analysis on tails snip samples while BL helped with data analysis and interpretation. LJ and EAM completed the statistical analysis and developed the idea of the paper. LJ wrote the manuscript and all other authors revised and edited the manuscript.

COMPETING INTERESTS

The authors declare no competing interests.

SUPPLEMENTARY MATERIAL

See supplementary materal at [] for access to supplementary figures and tables.

REFERENCES

Anbuhl, K.L., Benichoux, V., Greene, N.T., Brown, A.D., Tollin, D.J., 2017. Development of the head, pinnae, and acoustical cues to sound location in a precocial species, the guinea pig (Cavia porcellus). Hearing Research 356, 35–50. https://doi.org/10.1016/j.heares.2017.10.015

Arnold: The auditory brainstem response - Google Scholar, n.d.

Backoff, P.M., Caspary, D.M., 1994. Age-related changes in auditory brainstem responses in fischer 344 rats: effects of rate and intensity. Hearing Research 73, 163–172. https://doi.org/10.1016/0378-5955(94)90231-3

Barker, A.J., Koch, U., Lewin, G.R., Pyott, S.J., 2021. Hearing and Vocalizations in the Naked Mole-Rat, in: Buffenstein, R., Park, T.J., Holmes, M.M. (Eds.), The Extraordinary Biology of the Naked Mole-Rat. Springer International Publishing, Cham, pp. 157–195. https://doi.org/10.1007/978-3-030-65943-1_6

Bates, D., Mächler, M., Bolker, B., Walker, S., 2014. Fitting Linear Mixed-Effects Models using lme4. https://doi.org/10.48550/ARXIV.1406.5823

Bedford, N.L., Hoekstra, H.E., 2015. Peromyscus mice as a model for studying natural variation. eLife 4, e06813. https://doi.org/10.7554/eLife.06813

Benichoux, V., Ferber, A., Hunt, S., Hughes, E., Tollin, D., 2018. Across Species "Natural Ablation" Reveals the Brainstem Source of a Noninvasive Biomarker of Binaural Hearing. J. Neurosci. 38, 8563–8573. https://doi.org/10.1523/JNEUROSCI.1211-18.2018

Blauert, J., 1997. Spatial Hearing: The Psychophysics of Human Sound Localization. MIT Press.

Bradley, R.D., Durish, N.D., Rogers, D.S., Miller, J.R., Engstrom, M.D., Kilpatrick, C.W., 2007. Toward a Molecular Phylogeny for Peromyscus: Evidence from Mitochondrial Cytochrome-b Sequences. Journal of Mammalogy 88, 1146–1159. https://doi.org/10.1644/06-MAMM-A-342R.1

Brittan-Powell, E.F., Dooling, R.J., 2004. Development of auditory sensitivity in budgerigars (*Melopsittacus undulatus*). The Journal of the Acoustical Society of America 115, 3092–3102. https://doi.org/10.1121/1.1739479

Burger, J., Gochfeld, M., 1992. Survival and reproduction in Peromyscus leucopus in the laboratory: viable model for aging studies. Growth Dev Aging 56, 17–22.

Caire, W., 1989. Mammals of Oklahoma. University of Oklahoma Press.

Capshaw, G., Brown, A.D., Peña, J.L., Carr, C.E., Christensen-Dalsgaard, J., Tollin, D.J., Womack, M.C., McCullagh, E.A., 2023. The continued importance of comparative auditory research to modern scientific discovery. Hearing Research 433, 108766. https://doi.org/10.1016/j.heares.2023.108766

Capshaw, G., Vicencio-Jimenez, S., Screven, L.A., Burke, K., Weinberg, M.M., Lauer, A.M., 2022. Physiological Evidence for Delayed Age-related Hearing Loss in Two Long-lived Rodent Species (Peromyscus leucopus and P. californicus). JARO 23, 617–631. https://doi.org/10.1007/s10162-022-00860-4

Charlton, B.D., Owen, M.A., Swaisgood, R.R., 2019. Coevolution of vocal signal characteristics and hearing sensitivity in forest mammals. Nat Commun 10, 2778. https://doi.org/10.1038/s41467-019-10768-y

Chawla, A., McCullagh, E.A., 2022. Auditory Brain Stem Responses in the C57BL/6J Fragile X Syndrome-Knockout Mouse Model. Frontiers in Integrative Neuroscience 15.

Childs, J.E., Ksiazek, T.G., Spiropoulou, C.F., Krebs, J.W., Morzunov, S., Maupin, G.O., Gage, K.L., Rollin, P.E., Sarisky, J., Enscore, R.E., Frey, J.K., Peters, C.J., Nichol, S.T., 1994.

Serologic and Genetic Identification of Peromyscus maniculatus as the Primary Rodent Reservoir for a New Hantavirus in the Southwestern United States. Journal of Infectious Diseases 169, 1271–1280. https://doi.org/10.1093/infdis/169.6.1271

Choate, J.R., 1973. Identification and Recent Distribution of White-Footed Mice (Peromyscus) in New England. Journal of Mammalogy 54, 41–49. https://doi.org/10.2307/1378871

Colburn, H.S., Zurek, P.M., Durlach, N.I., 1987. Binaural Directional Hearing—Impairments and Aids, in: Yost, W.A., Gourevitch, G. (Eds.), Directional Hearing, Proceedings in Life Sciences. Springer, New York, NY, pp. 261–278. https://doi.org/10.1007/978-1-4612-4738-8_11

Csiszar, A., Labinskyy, N., Zhao, X., Hu, F., Serpillon, S., Huang, Z., Ballabh, P., Levy, R.J., Hintze, T.H., Wolin, M.S., Austad, S.N., Podlutsky, A., Ungvari, Z., 2007. Vascular superoxide and hydrogen peroxide production and oxidative stress resistance in two closely related rodent species with disparate longevity. Aging Cell 6, 783–797. https://doi.org/10.1111/j.1474-9726.2007.00339.x

Cummings, J.R., Vessey, S.H., 1994. Agricultural Influences on Movement Patterns of White-Footed Mice (Peromyscus leucopus). The American Midland Naturalist 132, 209–218. https://doi.org/10.2307/2426575

Dammann, P., 2017. Slow aging in mammals—Lessons from African mole-rats and bats. Seminars in Cell & Developmental Biology, Science communication in the field of fundamental biomedical research 70, 154–163. https://doi.org/10.1016/j.semcdb.2017.07.006

Dice, L.R., Barto, E., 1952. Ability of Mice of the Genus Peromyscus to Hear Ultrasonic Sounds. Science 116, 110–111. https://doi.org/10.1126/science.116.3005.110

Ducroz, J.F., Volobouev, V., Granjon, L., 2001. An Assessment of the Systematics of Arvicanthine Rodents Using Mitochondrial DNA Sequences: Evolutionary and Biogeographical Implications. Journal of Mammalian Evolution 8, 173–206. https://doi.org/10.1023/A:1012277012303

Ehret, G., Dreyer, A., 1984. Localization of tones and noise in the horizontal plane by unrestrained house mice (Mus musculus). Journal of Experimental Biology 109, 163–174. https://doi.org/10.1242/jeb.109.1.163

Fairbairn, D.J., 1977. The spring decline in deer mice: death or dispersal? Can. J. Zool. 55, 84–92. https://doi.org/10.1139/z77-009

Fiset, J., Tessier, N., Millien, V., Lapointe, F.-J., 2015. Phylogeographic Structure of the White-Footed Mouse and the Deer Mouse, Two Lyme Disease Reservoir Hosts in Québec. PLoS ONE 10, e0144112. https://doi.org/10.1371/journal.pone.0144112

Gessele, N., Garcia-Pino, E., Omerbašić, D., Park, T.J., Koch, U., 2016. Structural Changes and Lack of HCN1 Channels in the Binaural Auditory Brainstem of the Naked Mole-Rat (Heterocephalus glaber). PLOS ONE 11, e0146428. https://doi.org/10.1371/journal.pone.0146428

Goksoy, C., Demirtas, S., Yagcioglu, S., Ungan, P., 2005. Interaural delay-dependent changes in the binaural interaction component of the guinea pig brainstem responses. Brain Research 1054, 183–191. https://doi.org/10.1016/j.brainres.2005.06.083

Grothe, B., Pecka, M., McAlpine, D., 2010. Mechanisms of sound localization in mammals. Physiol Rev 90, 983–1012. https://doi.org/10.1152/physrev.00026.2009

Guo, Z., Wang, M., Tian, G., Burger, J., Gochfeld, M., Yang, C.S., 1993. Age- and gender-related variations in the activities of drug-metabolizing and antioxidant enzymes in the white-footed mouse (Peromyscus leucopus). Growth Dev Aging 57, 85–100.

Hackney, S., Stancampiano, A.J., 2015. Microhabitat Preferences of a Small Mammal Assemblage in Canadian County, Oklahoma. Proceedings of the Oklahoma Academy of Science 95.

Harney, B.A., Dueser, R.D., 1987. Vertical Stratification of Activity of Two Peromyscus Species: An Experimental Analysis. Ecology 68, 1084–1091. https://doi.org/10.2307/1938380

Heeringa, A.N., Zhang, L., Ashida, G., Beutelmann, R., Steenken, F., Köppl, C., 2020. Temporal Coding of Single Auditory Nerve Fibers Is Not Degraded in Aging Gerbils. J. Neurosci. 40, 343–354. https://doi.org/10.1523/JNEUROSCI.2784-18.2019

Heffner, H.E.H., Rickye S., 2001. Behavioral Assessment of Hearing in Mice, in: Handbook of Mouse Auditory Research. CRC Press.

Heffner, R.S., Heffner, H.E., 1993. Degenerate hearing and sound localization in naked mole rats (*Heterocephalus glaber*), with an overview of central auditory structures. J of Comparative Neurology 331, 418–433. https://doi.org/10.1002/cne.903310311

Heffner, R.S., Heffner, H.E., 1992. Hearing and sound localization in blind mole rats (*Spalax ehrenbergi*). Hearing Research 62, 206–216. https://doi.org/10.1016/0378-5955(92)90188-S

Heffner, R.S., Heffner, H.E., 1990. Vestigial hearing in a fossorial mammal, the pocket gopher (*Geomys bursarius*). Hearing Research 46, 239–252. https://doi.org/10.1016/0378-5955(90)90005-A

Heffner, R.S., Heffner, H.E., 1982. Hearing in the elephant (Elephas maximus): absolute sensitivity, frequency discrimination, and sound localization. J Comp Physiol Psychol 96, 926–944.

Heffner, R.S., Koay, G., Heffner, H.E., 2020. Hearing and sound localization in Cottontail rabbits, Sylvilagus floridanus. J Comp Physiol A 206, 543–552. https://doi.org/10.1007/s00359-020-01424-8

Heffner, R.S., Koay, G., Heffner, H.E., 2001. Audiograms of five species of rodents: implications for the evolution of hearing and the perception of pitch. Hearing Research 157, 138–152. https://doi.org/10.1016/S0378-5955(01)00298-2

Houseknecht, C.R., 1968. Sonographic Analysis of Vocalizations of Three Species of Mice. Journal of Mammalogy 49, 555. https://doi.org/10.2307/1378232

Jones, S.J., Van der Poel, J.C., 1990. Binaural interaction in the brain-stem auditory evoked potential: evidence for a delay line coincidence detection mechanism. Electroencephalography and Clinical Neurophysiology/Evoked Potentials Section 77, 214–224. https://doi.org/10.1016/0168-5597(90)90040-K

Jüchter, C., Beutelmann, R., Klump, G.M., 2022. Speech sound discrimination by Mongolian gerbils. Hearing Research 418, 108472. https://doi.org/10.1016/j.heares.2022.108472

Karino, S., Smith, P.H., Yin, T.C.T., Joris, P.X., 2011. Axonal Branching Patterns as Sources of Delay in the Mammalian Auditory Brainstem: A Re-Examination. J. Neurosci. 31, 3016–3031. https://doi.org/10.1523/JNEUROSCI.5175-10.2011

Kidd, G., Mason, C.R., Rohtla, T.L., 1995. Binaural advantage for sound pattern identification. The Journal of the Acoustical Society of America 98, 1977–1986. https://doi.org/10.1121/1.414459

King, J.A., 1968. Biology of Peromyscus (Rodentia). Biology of Peromyscus (Rodentia).

Kirkland, G.L., Layne, J.N., 1989. Advances in the Study of Peromyscus (Rodentia) Texas Tech University Press. Lubbock, TX.

Labinskyy, N., Mukhopadhyay, P., Toth, J., Szalai, G., Veres, M., Losonczy, G., Pinto, J.T., Pacher, P., Ballabh, P., Podlutsky, A., Austad, S.N., Csiszar, A., Ungvari, Z., 2009. Longevity is associated with increased vascular resistance to high glucose-induced oxidative stress and inflammatory gene expression in Peromyscus leucopus. American Journal of Physiology-Heart and Circulatory Physiology 296, H946–H956. https://doi.org/10.1152/ajpheart.00693.2008

Larson, S.R., Lee, X., Paskewitz, S.M., 2018. Prevalence of Tick-Borne Pathogens in Two Species of Peromyscus Mice Common in Northern Wisconsin. Journal of Medical Entomology 55, 1002–1010. https://doi.org/10.1093/jme/tjy027

Lauer, A.M., Engel, J.H., Schrode, K., 2018. Rodent Sound Localization and Spatial Hearing, in: Dent, M.L., Fay, R.R., Popper, A.N. (Eds.), Rodent Bioacoustics, Springer Handbook of Auditory Research. Springer International Publishing, Cham, pp. 107–130. https://doi.org/10.1007/978-3-319-92495-3_5

Laumen, G., Ferber, A.T., Klump, G.M., Tollin, D.J., 2016a. The Physiological Basis and Clinical Use of the Binaural Interaction Component of the Auditory Brainstem Response. Ear Hear 37, e276–e290. https://doi.org/10.1097/AUD.0000000000000301

Laumen, G., Tollin, D.J., Beutelmann, R., Klump, G.M., 2016b. Aging effects on the binaural interaction component of the auditory brainstem response in the Mongolian gerbil: Effects of interaural time and level differences. Hearing Research 337, 46–58. https://doi.org/10.1016/j.heares.2016.04.009

Lewarch, C.L., Hoekstra, H.E., 2018. The evolution of nesting behaviour in Peromyscus mice. Animal Behaviour 139, 103–115. https://doi.org/10.1016/j.anbehav.2018.03.008

Light, J.E., Siciliano-Martina, L., Dohlanik, E.G., Hafner, D.J., Lawing, A.M., Greenbaum, I.F., Light, J.E., Siciliano-Martina, L., Dohlanik, E.G., Hafner, D.J., Lawing, A.M., Greenbaum, I.F., 2021. Morphological differentiation of Peromyscus leucopus and P. maniculatus in East Texas. Therya 12, 369–387. https://doi.org/10.12933/therya-21-1116

McCullagh, E.A., Peacock, J., Lucas, A., Poleg, S., Greene, N.T., Gaut, A., Lagestee, S., Zhang, Y., Kaczmarek, L.K., Park, T.J., Tollin, D.J., Klug, A., 2022. Auditory brainstem development of naked mole-rats (Heterocephalus glaber). Proceedings of the Royal Society B: Biological Sciences 289, 20220878. https://doi.org/10.1098/rspb.2022.0878

McCullagh, E.A., Poleg, S., Greene, N.T., Huntsman, M.M., Tollin, D.J., Klug, A., 2020. Characterization of Auditory and Binaural Spatial Hearing in a Fragile X Syndrome Mouse Model. eNeuro 7. https://doi.org/10.1523/ENEURO.0300-19.2019

Miller, J.R., Engstrom, M.D., 2012. Vocal stereotypy in the rodent genera Peromyscus and Onychomys (Neotominae): taxonomic signature and call design. Bioacoustics 21, 193–213. https://doi.org/10.1080/09524622.2012.675176

Millien, V., Ledevin, R., Boué, C., Gonzalez, A., 2017. Rapid morphological divergence in two closely related and co-occurring species over the last 50 years. Evol Ecol 31, 847–864. https://doi.org/10.1007/s10682-017-9917-0

Mills, J.H., Schmiedt, R.A., Kulish, L.F., 1990. Age-related changes in auditory potentials of mongolian gerbil. Hearing Research 46, 201–210. https://doi.org/10.1016/0378-5955(90)90002-7

Moore, E.J., 1983. Bases of auditory brain-stem evoked responses. Grune & Stratton.

Neil J. Ingham, S.K.T., Spiro D. Comis, Deborah J. Withington, 1998. The Auditory Brainstem Response of Aged Guinea Pigs. Acta Oto-Laryngologica 118, 673–680. https://doi.org/10.1080/00016489850183160

New, E.M., Hurd, J.A., Alarcon, G.A., Miller, C.S., Williams, P.A., Greene, N.T., Sergott, C.E., Li, B.-Z., Lei, T.C., McCullagh, E.A., 2024. Hearing ability of prairie voles (Microtus ochrogaster). J Acoust Soc Am 155, 555–567. https://doi.org/10.1121/10.0024357

Nicolas, V., Schaeffer, B., Missoup, A.D., Kennis, J., Colyn, M., Denys, C., Tatard, C., Cruaud, C., Laredo, C., 2012. Assessment of Three Mitochondrial Genes (16S, Cytb, CO1) for Identifying Species in the Praomyini Tribe (Rodentia: Muridae). PLOS ONE 7, e36586. https://doi.org/10.1371/journal.pone.0036586

Ohlemiller, K.K., Frisina, R.D., 2008. Age-Related Hearing Loss and Its Cellular and Molecular Bases, in: Schacht, J., Popper, A.N., Fay, R.R. (Eds.), Auditory Trauma, Protection, and Repair, Springer Handbook of Auditory Research. Springer US, Boston, MA, pp. 145–194. https://doi.org/10.1007/978-0-387-72561-1_6

Ordóñez-Garza, N., Matson, J.O., Strauss, R.E., Bradley, R.D., Salazar-Bravo, J., 2010. Patterns of phenotypic and genetic variation in three species of endemic Mesoamerican Peromyscus (Rodentia: Cricetidae). Journal of Mammalogy 91, 848–859. https://doi.org/10.1644/09-MAMM-A-167.1

Pasch, B., Tokuda, I.T., Riede, T., 2017. Grasshopper mice employ distinct vocal production mechanisms in different social contexts. Proc. R. Soc. B. 284, 20171158. https://doi.org/10.1098/rspb.2017.1158

Platt, R.N., II, Amman, B.R., Keith, M.S., Thompson, C.W., Bradley, R.D., 2015. What Is Peromyscus? Evidence from nuclear and mitochondrial DNA sequences suggests the need for a new classification. Journal of Mammalogy 96, 708–719. https://doi.org/10.1093/jmammal/gyv067

Pomerantz, S.M., Clemens, L.G., 1981. Ultrasonic vocalizations in male deer mice (Peromyscus maniculatus bairdi): Their role in male sexual behavior. Physiology & Behavior 27, 869–872. https://doi.org/10.1016/0031-9384(81)90055-X

Ralls, K., 1967. Auditory sensitivity in mice: Peromyscus and Mus musculus. Animal Behaviour 15, 123–128. https://doi.org/10.1016/S0003-3472(67)80022-8

Ramsier, M.A., Dominy, N.J., 2010. A comparison of auditory brainstem responses and behavioral estimates of hearing sensitivity in Lemur catta and Nycticebus coucang. American Journal of Primatology 72, 217–233. https://doi.org/10.1002/ajp.20780

Riede, T., Kobrina, A., Bone, L., Darwaiz, T., Pasch, B., 2022. Mechanisms of sound production in deer mice (Peromyscus spp.). Journal of Experimental Biology 225, jeb243695. https://doi.org/10.1242/jeb.243695

Riedel, H., Kollmeier, B., 2006. Interaural delay-dependent changes in the binaural difference potential of the human auditory brain stem response. Hearing Research 218, 5–19. https://doi.org/10.1016/j.heares.2006.03.018

Rieger, N.S., Marler, C.A., 2018. The function of ultrasonic vocalizations during territorial defence by pair-bonded male and female California mice. Animal Behaviour 135, 97–108. https://doi.org/10.1016/j.anbehav.2017.11.008

Robins, J.H., Hingston, M., Matisoo-Smith, E., Ross, H.A., 2007. Identifying *Rattus* species using mitochondrial DNA. Molecular Ecology Notes 7, 717–729. https://doi.org/10.1111/j.1471-8286.2007.01752.x

Russell, L., 2018. Emmeans: estimated marginal means, aka least-squares means. R package version 1.

Sayers, E.W., Bolton, E.E., Brister, J.R., Canese, K., Chan, J., Comeau, D.C., Connor, R., Funk, K., Kelly, C., Kim, S., Madej, T., Marchler-Bauer, A., Lanczycki, C., Lathrop, S., Lu, Z., Thibaud-Nissen, F., Murphy, T., Phan, L., Skripchenko, Y., Tse, T., Wang, J., Williams, R., Trawick, B.W., Pruitt, K.D., Sherry, S.T., 2022. Database resources of the National Center for Biotechnology Information. Nucleic Acids Research 50, D20. https://doi.org/10.1093/nar/gkab1112

Sayers, E.W., Cavanaugh, M., Clark, K., Pruitt, K.D., Schoch, C.L., Sherry, S.T., Karsch-Mizrachi, I., 2021. GenBank. Nucleic Acids Research 49, D92–D96. https://doi.org/10.1093/nar/gkaa1023

Shi, Y., Pulliam, D.A., Liu, Y., Hamilton, R.T., Jernigan, A.L., Bhattacharya, A., Sloane, L.B., Qi, W., Chaudhuri, A., Buffenstein, R., Ungvari, Z., Austad, S.N., Van Remmen, H., 2013. Reduced mitochondrial ROS, enhanced antioxidant defense, and distinct age-related changes in oxidative damage in muscles of long-lived Peromyscus leucopus. American Journal of Physiology-Regulatory, Integrative and Comparative Physiology 304, R343–R355. https://doi.org/10.1152/ajpregu.00139.2012

Sikes, R.S., Gannon, W.L., the Animal Care and Use Committee of the American Society of Mammalogists, 2011. Guidelines of the American Society of Mammalogists for the use of wild mammals in research. Journal of Mammalogy 92, 235–253. https://doi.org/10.1644/10-MAMM-F-355.1

Sikes, R.S., the Animal Care and Use Committee of the American Society of Mammalogists, 2016. 2016 Guidelines of the American Society of Mammalogists for the use of wild mammals in research and education. Journal of Mammalogy 97, 663–688. https://doi.org/10.1093/jmammal/gyw078

Stancampiano, A.J., Schnell, G.D., 2004. Microhabitat Affinities of Small Mammals in Southwestern Oklahoma. Journal of Mammalogy 85, 948–958.

Suthakar, K., Liberman, M.C., 2019. A simple algorithm for objective threshold determination of auditory brainstem responses. Hearing Research 381, 107782. https://doi.org/10.1016/j.heares.2019.107782

Suzuki, T., Horiuchi, K., 1981. Rise Time of Pure-Tone Stimuli in Brain Stem Response Audiometry. Audiology 20, 101–112. https://doi.org/10.3109/00206098109072688

Ungan, P., Yağcioğlu, S., Özmen, B., 1997. Interaural delay-dependent changes in the binaural difference potential in cat auditory brainstem response: implications about the origin of the binaural interaction component 1. Hearing Research 106, 66–82. https://doi.org/10.1016/S0378-5955(97)00003-8

Voelkl, B., Altman, N.S., Forsman, A., Forstmeier, W., Gurevitch, J., Jaric, I., Karp, N.A., Kas, M.J., Schielzeth, H., Van de Casteele, T., Würbel, H., 2020. Reproducibility of animal research in light of biological variation. Nat Rev Neurosci 21, 384–393. https://doi.org/10.1038/s41583-020-0313-3

Wang, Xin, Zhu, M., Samuel, O.W., Wang, Xiaochen, Zhang, H., Yao, J., Lu, Y., Wang, M., Mukhopadhyay, S.C., Wu, W., Chen, S., Li, G., 2020. The Effects of Random Stimulation Rate on Measurements of Auditory Brainstem Response. Frontiers in Human Neuroscience 14.

Wickham, H., 2016. Programming with ggplot2, in: Wickham, H. (Ed.), Ggplot2: Elegant Graphics for Data Analysis, Use R! Springer International Publishing, Cham, pp. 241–253. https://doi.org/10.1007/978-3-319-24277-4_12

Wolski, L.F., Anderson, R.C., Bowles, A.E., Yochem, P.K., 2003. Measuring hearing in the harbor seal (Phoca vitulina): Comparison of behavioral and auditory brainstem response techniques. The Journal of the Acoustical Society of America 113, 629–637. https://doi.org/10.1121/1.1527961

Zhou, X., Jen, P.H.-S., Seburn, K.L., Frankel, W.N., Zheng, Q.Y., 2006. Auditory brainstem responses in 10 inbred strains of mice. Brain Research 1091, 16–26. https://doi.org/10.1016/j.brainres.2006.01.107

Figure legends:

Figure 1: Map showing trapping site locations in Oklahoma. Packsaddle wildlife management area (WMA) sites are presented by yellow triangle, James Collin wildlife management area (WMA) sites are presented by blue squares, and Payne County sites are presented by red circle.

Figure 2: Morphological differences between *P. leucopus* and *P. maniculatus*. Pinnae, head, and body features (**A**) were evaluated between species (pink boxplot = *leucopus*, blue boxplot = *maniculatus*). Measurements JK show the inter pinnae distance, JN the nose to pinna distance, MK the pinna width, LM the pinna height, OP the tail length, and PQ the body length. Effective pinna diameter was calculated by taking the square root of pinna height multiplied by pinna width (MK/LM). Significant differences were observed for all features: Pinna width (**B**), Pinna length (**C**), Effective diameter (**D**), Nose to pinna distance (**E**), Inter pinna distance (**F**), Body length (**G**), Tail length (**H**), and Body mass (**I**). Peromyscus head image (**A**) was captured inone of our sampling site, not an animal that was measured in this current study. Image is presented only for demonstration of measurements.

Figure 3: Figure 3A and 3B show auditory brainstem response patterns of a female *P. leucopus* and a female *P. maniculatus*, respectively determined with clicks of different intensities in a fixed scale. Main wave components are intentified I through V in the 90 dB SPL examples. The species names are shown at the top of each ABR trace. Hearing range was measured across frequency (1-64 kHz) for both *P. leucopus* and *P. maniculatus* (Figure 3C). No significant main effects of frequency between species were found. Unfilled blue circles represent *P. maniculatus* while filled pink squares represent *P. leucopus*. The vertical bars represent the standard error at each frequency.

Figure 4: Average amplitude of wave I and wave IV of auditory brainstem responses determined with clicks of different intensities (pink filled square = *P. leucopus* (n = 15), blue unfilled circle = *P. maniculatus* (n = 11)). The average wave IV/I amplitude ratio at each intensity is shown in figure 4E. The vertical bars represent the standard error at each point. Significant main effects of intensity on wave I and IV amplitude were detected for each species.

Figure 5: Average peak latency of wave I and wave IV of auditory brainstem responses determined with clicks of different intensities (Pink filled squares = *P. leucopus* (n = 15), Blue unfilled circles= *P. maniculatus* (n = 11)). The average wave I-IV inter-peak latency at each intensity is shown in 5E. The vertical bars represent the standard error at each point.

Figure 6: Binaural ABRs in wild *P. leucopus* (pink filled square) and *P. maniculatus* (blue unfilled circle). 6A, Shift in DN1 latency (ms) relative to ITD; reference latency at ITD = 0 is set to 0 ms. 6B, percentage relative DN1 amplitude relative to ITD normalized to the DN1 amplitude for ITD = 0 ms. Relative amplitude and latency of the DN1 BIC with varying ITD between - 2 to + 2 ms in 0.5 ms steps were measured. Significant main effects of ITDs and species were detected in BIC shift in DN1 latencies between both species. No significant main effect of species was observed between both species for relative amplitude of the BIC across ITDs.

Table 1: Age was estimated based on body mass for each species based on published literature. Ages for *P. maniculatus* was describe as follows: Juveniles < 14 g, subadults, between 14-17 grams, and adults, > 17 g (Fairbairn, 1977). We inferred ages for *P. leucopus* as follows: Juveniles < 13 g, subadults, between 13 – 18 g, and adults > 18 grams (Cummings and Vessey, 1994). We did not make comparisons by ages due to limited sample sizes by age groups.

Table 2: Morphological characteristics features of *P. maniculatus* and *P. leucopus* of the Packsaddle wildlife management area (WMA), James Collin wildlife management area (WMA) and Payne County. Values presented represent the mean of different morphological features recorded, the degrees of freedom, F-statistic and p-value of morphological differences between species.